Ion channel of acetylcholine receptor reconstructed from images of postsynaptic membranes

Chikashi Toyoshima & Nigel Unwin

Medical Research Council Laboratory of Molecular Biology, Hills Road, Cambridge CB2 2QH, UK

The nicotinic acetylcholine receptor belongs to a class of molecules that respond transiently to chemical stimuli by opening a water-filled channel through the cell membrane for cations to diffuse. This channel lies along the central axis delineated by a ring of five homologous, membrane-spanning subunits[1,2] and thus has properties, such as conductance and ion selectivity, which depend on the profile created by the encircling subunits. Insight has been gained recently about the amino-acid residues implicated directly in the ion transport[3–7], and some information about the subunit configuration around the channel has come from electron microscopy studies of postsynaptic membranes crystallized in the form of flattened tubular vesicles[8–11]. The resolution along the axis of the channel has, however, been limited by the restricted range of views obtainable. Here we report the structure of the channel at 17 Å resolution, determined by three-dimensional image reconstruction from tubular vesicles having receptors organized in helical arrays across their surfaces. The helical symmetry is preserved by suspending the tubes in thin films of ice, and the receptors in such tubes can be seen from all angles, allowing the channel to be revealed clearly in relation to the lipid bilayer and the peripheral protein for the first time.

The long and narrow tubes were obtained for this study (Fig. 1*a*) from postsynaptic membranes of the electric ray, *Torpedo marmorata*, and consist of dimers of receptor molecules periodically arranged in the native lipids[8]. Before investigating the helical structure, we first examined features in thin sections (Fig. 1*b*). The tubes, like isolated fragments of postsynaptic membranes[12,13], contain peripheral proteins, seen as a uniformly thick layer decorating their inner surface. These proteins probably consist predominantly of the protein of relative molecular mass 43,000 (43K) (refs 14–16), which associates weakly with the receptor and is released from the membranes (unless treated with *N*-ethylmaleimide[17]) by alkaline *p*H[18]. The proteins coat more than 50% of the inner surfaces of the tubes, assuming that the very thin layer of stain sometimes observed beneath the membrane (Fig. 1*b*, lower left) corresponds only to the receptor. Moreover, we find (Fig. 1*b*, right) that the proteins redistribute in an irregular way on the surface after short exposure to alkaline *p*H. Because of *N*-ethylmaleimide treatment[10,17], they are not released and the ordered arrangement of the receptors is not significantly disturbed. Thus the tubes have different cytoplasmic structures at different *p*Hs, providing a means to distinguish the receptor and peripheral protein components from one another.

For the reconstructions we recorded images of the frozen tubes (Fig. 1*a*) in weakly and then strongly defocused pairs[19]. Diffraction patterns of these images (Fig. 2*a*) show a series of layer lines characteristic of a helical structure and extending to a resolution of ~16 Å. Three-dimensional maps were calculated from layer-line data summed from both images (Fig. 2*b*), and represent information averaged over about 4,000 molecules.

Figure 3*a* shows a section normal to the tube axis in the three-dimensional map obtained for the native tubes. The receptors form an oblique lattice on the cylindrical surface so that this section intercepts several of them in different places. Two circumferential weakly contrasted bands are also present; the walls of the channel made by the synaptic portion of the receptor project ~65 Å from the outermost band, whereas cytoplasmic densities extend ~55 Å from the innermost band.

The two bands must be a feature of the lipid bilayer. First, they are at the same radii in relation to the rest of the structure, as the edges of the membrane seen clearly in the thin sections (Fig. 3*a*, insert). Second, their separation (30 Å) is identical to that measured from images of receptor-containing vesicles, also present in the same preparation (results not shown). Third, the bands are at the same radii as those regions of the structure where the contrast between the protein and the outside environment is weakest (Fig. 2*c*). This finding is anticipated because the density of the protein should be matched by the phospholipid headgroups and steroid moiety of the cholesterol in the outer

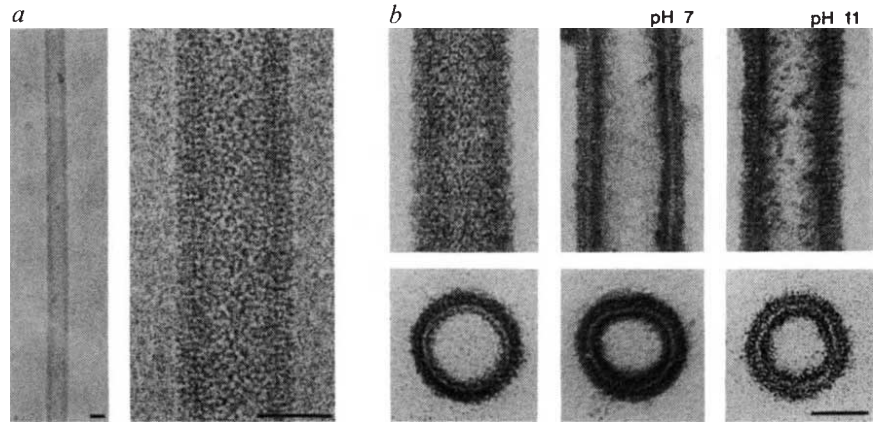

Fig. 1 Images of tubes suspended in ice (*a*), and embedded in plastic and sectioned (*b*). The sections are of the tubes cut longitudinally (upper row) and transversely (lower row), the membrane appearing as a thin white line. The longitudinal sections are of the tube surface (left), showing the good preservation of receptors, and of regions just below the surface before (middle) and after (right) exposure to alkaline *p*H. The transverse sections are of the native (left, middle) and alkali-treated (right) tubes. The protein coat, indicated by the uniformly thick layer of stain lining the inner membrane surface, is sometimes missing (lower left), despite the well preserved structure outside the membrane. This coat, where present, is disrupted and reorganized in an irregular way by the alkaline *p*H (right); as the receptors retain their position in the crystal lattice, the coat must represent non-receptor protein. Scale bar, 500 Å.

Methods. Tubes for the helical analysis, as in *a*, were maintained in 100 mM sodium cacodylate, *p*H 6.8, or dialysed against 100 mM sodium phosphate, *p*H 11.0, immediately before freezing. The freezing was performed by plunging holey carbon grids, to which the specimens had been applied, into liquid ethane slush. Electron microscopy was at 120 kV, using a Philips EM400T or EM420 equipped with a low-dose kit and Gatan cryo-holder, maintained at −168 °C. Images were recorded of tubes over holes in the carbon support film (magnification, ×36,000; dose, ~8 electrons $Å^{-2}$), at ~8,000 Å then ~20,000 Å underfocus[19] using Kodak SO163 film. Tube diameters had to be <750 Å to maintain helical symmetry. For the sectioned specimens, suspensions of the tubes in 100 mM sodium cacodylate were dialysed against sodium phosphate buffer either at *p*H 7.0 or *p*H 11.0 (4 °C, 40 min) and subsequently against fixative: 0.8% tannic acid (Mallenkrodt), 4.0% glutaraldehyde and 100 mM sodium phosphate, *p*H 7.0 (1 h); fixative was then mixed directly (1 : 1) with the suspension (30 min); specimens were pelleted, washed, reacted with 1% osmium tetroxide and embedded in the usual way; sections were post-stained with uranyl acetate and lead citrate.

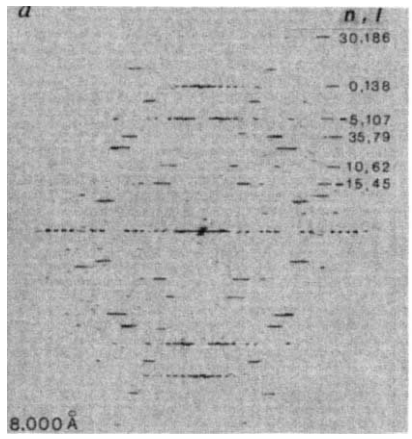

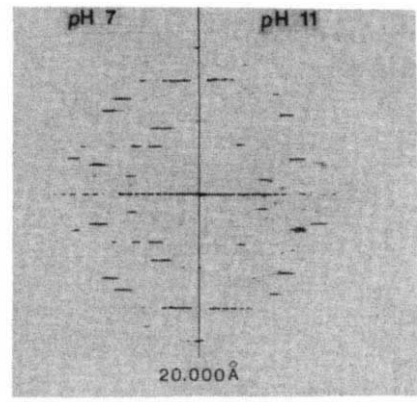

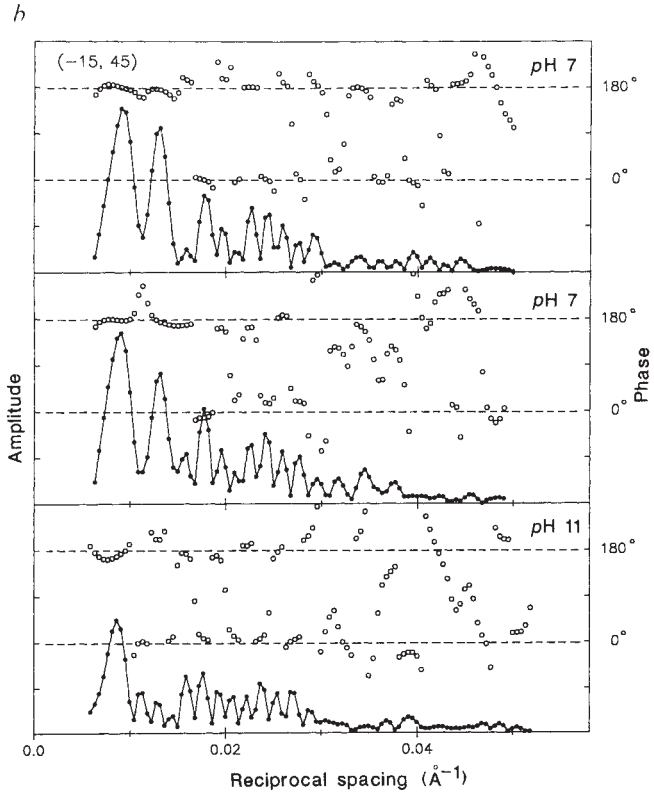

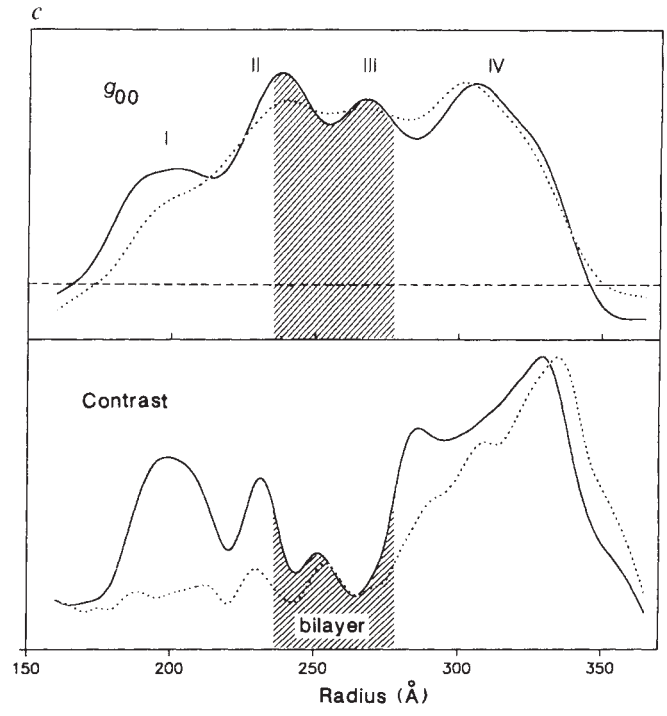

part of the bilayer[20] more nearly than by the low-density hydrocarbon chains in the inner part or by the surrounding ice.

The outer and inner leaflets of a lipid bilayer have not previously been resolved in electron image reconstructions, and the peak-to-peak separation of 30 Å is 10–15 Å smaller than might have been anticipated on the basis of profile X-ray diffraction measurements from typical biological membranes[20] or details seen in cryo-images of pure phospholipid vesicles[21]. Two factors could contribute to the smaller spacing observed. First, the scattering properties of electrons are different from those of X-rays: the oxygen and phosphorus atoms in the headgroup regions will be less emphasized by the electrons as the electron-scattering amplitudes for these atoms, relative to carbon atoms, are smaller than for X-rays[22]. Second, the postsynaptic membrane lipids contain a high proportion of cholesterol (almost 50 mol%[23]) which is intercalated between the phospholipid fatty acid chains. The denser steroid portions of these molecules are about 30 Å apart and contribute strongly to the X-ray diffraction profile[20]. Therefore, the appearance of the postsynaptic membrane in the electron images is probably dominated by the cholesterol, rather than by the phospholipids. To check on this interpretation we prepared artificial vesicles of dipalmitoyl phosphatidylcholine (the major phospholipid component of the postsynaptic membrane[23]) and demonstrated that the peak-to-peak separation in the cholesterol-free bilayer is much larger (>40 Å; data not shown).

Figure 3*b* shows another view of the native tube, from the inside, made by stacking cylindrical sections at successive radii on top of one another. At the outermost radii (most distant from the observer), the densities corresponding to the five receptor subunits all begin at about the same level, symmetrically encircling the ~25-Å-wide synaptic entrance to the channel. They follow paths that are almost parallel to the axis of the molecule throughout most of their length, passing through the lipid bilayer and emerging as five symmetrically disposed densities on the cytoplasmic side. These densities project 15–20 Å from the estimated position of the phospholipid headgroups. At smaller radii, the densities are replaced by a single, central density. The change in structure, from approximately pentagonal to a single density, is abrupt, as reflected by the two well separated peaks in the contrast plot (Fig. 2*c*).

◀ **Fig. 2** Diffraction patterns computed from images of the ice-embedded tubes (*a*), plots of amplitude and phase variations along a typical layer-line (*b*), and variations in radial density and contrast (*c*). The upper diffraction pattern is of a tube imaged at 8,000 Å underfocus (the first image of the pair; the indices *n* and *l* refer to the Bessel orders and layer-line numbers); the lower diffraction pattern (20,000 Å underfocus) is a composite comparing data from the native (left) and alkali-treated tubes (right); the layer-lines are not at identical levels on the two sides because of small differences in the unit cell of the surface lattice. The layer-line plots (*b*) show the amplitude and phase variations as a function of reciprocal spacing along the (−15, 45) layer-line; the three examples compare data used for the native map (average of ~4,000 molecules; upper), a second set of unused data (average of ~1,500 molecules; middle) and data for the high *p*H map (average of ~4,000 molecules; lower); this layer line corresponds to the (1, 0) reflection in analyses of the flattened tubes[8–11]; the transforms have been shifted to a common twofold origin, so that the phases would ideally be 0 or 180°; note that the first 10 major peaks in the upper two plots all have similar amplitudes and identical phases, whereas the equivalent peaks in the plot from the alkali-treated tubes show substantial differences; for example, the second peak (reciprocal spacing, 0.013 $Å^{-1}$) has a much weaker amplitude and an opposite phase to the corresponding peak from the native tubes. The variations in mean radial density g_{00} (*c*, upper) and contrast (*c*, lower) are across tubes frozen at *p*H 7 (full lines) and *p*H 11 (dotted lines). In the density plots (*c*, upper), peaks I and IV correspond to structures on the cytoplasmic and synaptic sides of the lipid bilayer respectively; peaks II and III correspond to the circumferential bands (Fig. 3*a*, *c*) associated with the bilayer; these curves, calculated from the composite equatorial layer-line data, relate closely to the edge profile in the images (as in Fig. 1*a* for example) seen by viewing the tubes at a glancing angle along their axes; the peak positions were shown not to be affected by the defocus level or by contrast transfer function correction. The contrast plots (*c*, lower) represent the differences between minimum and maximum densities at various levels throughout the two three-dimensional maps. The regions of weakest contrast, in the bilayer-spanning portion of the structure, are at the same radii as peaks II and III above, indicating that the protein and the bilayer in these regions have almost matching densities; the extent of the bilayer to the estimated positions of the phospholipid headgroups is indicated by the shaded area. On the cytoplasmic side of the bilayer (radius, 190–245 Å) the native structure shows two regions in which features are well contrasted, one (radius, 190–225 Å) associated with the peripheral protein, and the other (radius, 225–245 Å) associated with the part of the receptor projecting from the phospholipid headgroups; in the alkali-treated structure the contrast associated with the peripheral protein has disappeared, indicating a loss of regularity.

Methods. Appropriate areas were densitometered (scanning aperture and step size, 15 μm), converting the images into two-dimensional arrays of optical densities. Helical reconstruction methods, as outlined below, were different in several ways from those commonly used[29]. The image arrays were interpolated so that layer lines in the Fourier transforms were in exact register with the sampling grid to provide accurate Fourier terms; for the interpolation, the repeat distance and the rotation of the tube relative to the array were measured by cross-correlating two different parts along the tube. Layer lines in Fourier transforms calculated from 512 × 1,024 image arrays (typically 4,000 Å long portions of the tube) were extracted and the two sides averaged to improve the signal-to-noise ratio. Further improvement in signal-to-noise ratio was achieved on the basis of the presence of twofold symmetry normal to the helix axis, and amplitude-weighted average phase deviations from the ideal values (0° or 180°) were used as a measure of the quality of the images. Refinement of the twofold phase origin, and the fitting of two images at different defocuses and of several stretches along the same tube were done in two steps. First, only strong layer lines were used to put different transforms to a common twofold origin. Then all the layer lines allowed by the selection rule were extracted to the cut-off resolution imposed by the defocus (~16 Å and ~30 Å for the weakly and strongly defocused images, respectively) and averaged. The phase residual for twofold symmetry was calculated for each layer line, which was discarded if the residual was >45°. These procedures allowed us to extract as much information as possible and provided significant improvement in the quality of the data: phase residuals for the twofold symmetry were 12–18° (strongly defocused image), 24–30° (weakly defocused image) before averaging, and were 15.6° (native; 36 layer-lines) and 19.9° (alkali-treated; 27 layer-lines) for the final composite datasets. Corrections were not made for the effects of non-uniform contrast transfer except along the equator, because the range in contrast transfer for the composite off-equatorial Fourier terms was small (0.4 for the lowest resolution terms, to 1.0); equatorial data were corrected assuming 7% amplitude contrast[19].

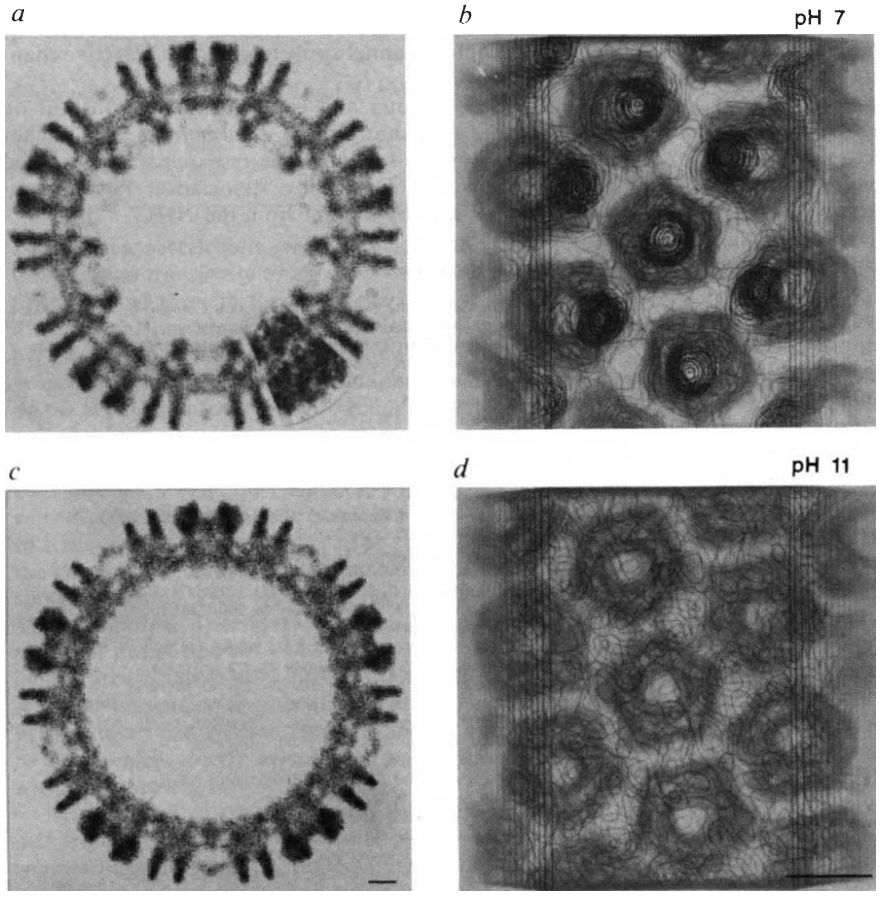

Fig. 3 Three-dimensional maps obtained by helical image reconstruction of the native tubes (*a*, *b*) and tubes at *p*H 11 (*c*, *d*); (*a*) and (*c*) are sections normal to the tube axis; (*b*) and (*d*) are views from the tube axis, looking outwards, made by stacking cylindrical sections at successive radii (spacing corresponding to 10 Å). The section (*a*) shows the lipid bilayer, the synaptic portion of the receptor projecting outwards, and the cytoplasmic portion and peripheral protein on the inside; a sector from a transverse thin section (Fig. 1*b*) is inserted to show the good correspondence in the position of the lipid bilayer visualized by the two methods; the outer diameter of the tube is ~700 Å. The view (*b*) shows the peripheral protein overlying the pentagonally symmetrical receptor at the cytoplasmic entrance, which projects just above the bilayer surface; the outermost contours enclose a total volume of ~310,000 $Å^3$ for the receptor and ~35,000 $Å^3$ for the peripheral protein; the volume for the receptor is about 85% of that expected for the glycosylated protein[30]. *c*, A section equivalent to that in *a* for the alkali-treated tubes (except for very slight differences in the units cells of the surface lattices); the lipid bilayer is not as clear, appearing to be slightly disrupted by the alkaline *p*H (ref. 31), and the densities lining the inner surface have changed. *d*, View equivalent to that in *b*, for the alkali-treated tubes showing the pentagonal outline made by the receptor subunits, but not the overlying peripheral protein. Scale bar, 50 Å.

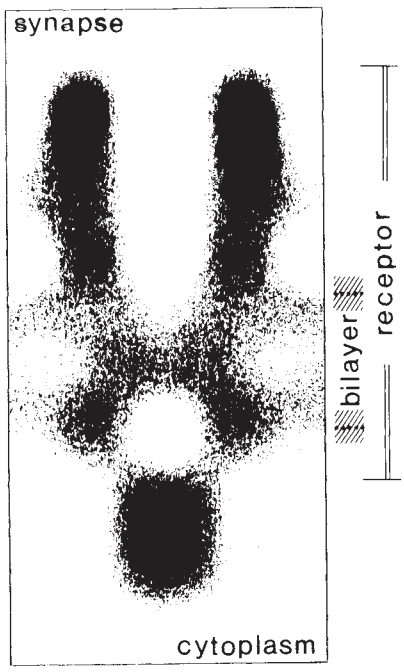

Fig. 4 Axial section through the cylindrically averaged native structure, showing details of the ion channel in relation to the lipid bilayer (estimated positions of the phospholipid headgroups indicated) and peripheral protein (bottom). The cylindrical averaging was done about the pseudo-fivefold axis of a single molecule.

Next, we analysed images of tubes frozen in alkaline solution, conditions which cause the peripheral protein to redistribute in an irregular way over the cytoplasmic surface (Fig. 1*b*) while the receptor retains its position in the crystal lattice. Diffraction patterns of these images were different, with marked changes along some of the layer lines (Fig. 2*a* and *b*). The three-dimensional map (Fig. 3*c* and *d*) reflected these changes: over the synaptic and bilayer-spanning portions, the structure was similar to the native one (Fig. 3*a*), but at the cytoplasmic end the central density, prominent in the native structure (Fig. 3*b*), was completely missing (Fig. 3*d*). Hence the central density, occupying a volume corresponding to about 30K, must be due to the peripheral protein. The location of the peripheral protein at the extremity of the receptor correlates well with the thin-section results (Fig. 1*b*) suggesting that the receptor projects only a small amount from the bilayer on the cytoplasmic side.

Although we have not directly identified the peripheral protein, it is reasonable to suppose that it corresponds to the 43K protein. The 43K protein is the only subsynaptic protein known to be present in concentrations similar to the receptor[15]; furthermore, morphological studies combined with antibody labelling have shown that the 43K protein does contribute extra density at the cytoplasmic end[24]. The redistribution over the membrane surface induced by the alkaline *p*H suggests that it could also be tethered to the lipid[16,25]. Various functions have been attributed to the 43K protein (refs 16 and 26); our findings lend support to a possible regulatory role.

The ion channel has several distinctive features, which are best illustrated with the structure obtained by cylindrically averaging the densities composing a single molecule about its pseudo-fivefold axis. Figure 4 is an axial section through the native structure. It shows the long vertical wall made by the encircling receptor subunits, the pair of transverse densities made by the lipid bilayer, and matter at the bottom of the receptor, identified as a peripheral protein rather than as a component of the receptor itself. This protein overlies the axial path of the channel, apparently touching some of the receptor subunits.

The ion channel at the synaptic end is about 25 Å across. It extends downwards towards the bilayer, changing little in cross-section over the next 60 Å. Then, close to the level of the outer phospholipid headgroups and over a very short distance, it becomes too narrow to be resolved (probably <10 Å diameter). The channel is unresolved across the interior of the bilayer, but at about the level of the inner phospholipid headgroups, it widens again, and continues with a wide (~20 Å diameter) cross-section to the cytoplasmic end, a further 15–20 Å away. The channel is partitioned quite sharply at the level of the phospholipid headgroups and may be considered to have a tripartite structure, consisting of two entrance domains and the 'pore' in between. We suggest that the three domains, and the short junctional regions, have specific roles in facilitating the flow of cations across the membrane. The entrance domains are tubular rather than funnel-shaped; their wall linings have a radius (10–13 Å) large enough to allow the ions to diffuse freely, but small enough in relation to the Debye distance[27] for surface charges to affect ion concentrations and thereby provide more efficient ion selectivity[28]. The junctions between the entrances and the pore form 'platforms', and charged residues located at these levels may act more directly in defining cation selectivity and the efficiency of transport. The pore itself is not resolved, but must have a much smaller radius than the entrance domains; presumably, it prevents the passage of large ions when agonist binds to induce the open state, and blocks ion flux altogether when the agonist is released.

Recent experiments, involving covalent labelling of the receptor with non-competitive channel blockers[3,4] and conductance measurements on chimaeric molecules[6], imply that at least a part of the putative α-helix M2 lines the pore. Details in the three-dimensional maps are in good accord with this possibility, as the pore appears to be about 30 Å long, roughly the length of the M2 helix; the charged amino acids that flank this helix could well be at the platforms bracketing the pore. It will be interesting to see if these structural characteristics of the acetylcholine receptor channel apply to other ion-selective channels as well.

We thank Dr C. Cazaux and colleagues at the Institut de Biologie Marine, Arcachon for *T. marmorata* and Nichol Thomson for cutting the sections. The research was supported in part by a Muscular Dystrophy Association Postdoctoral Fellowship to C.T. and by a grant from the NIH.

Received 15 August; accepted 4 October 1988.

1. Karlin, A. in *The Cell Surface and Neuronal Function* (eds Cotman, C. W., Poste, G. & Nicolson, G. L.) 191–260 (North-Holland, Amsterdam, 1980).
2. Changeux, J.-P., Devillers-Thiery, A. & Chemouille, P. *Science* **225,** 1335–1345 (1984).
3. Giraudat, J. *et al. Biochemistry* **26,** 2410–2418 (1987).
4. Hucho, F. W., Oberthur, W. & Lottspeich, F. *FEBS Lett.* **205,** 137–142 (1986).
5. Sakmann, B. *et. al. Nature* **318,** 538–543 (1985).
6. Imoto, K. *et al. Nature* **324,** 670–674 (1986).
7. Mishina, M. *et al. Nature* **313,** 364–369 (1985).
8. Brisson, A. & Unwin, P. N. T. *J. Cell Biol.* **99,** 1202–1211 (1984).
9. Brisson, A. & Unwin, P. N. T. *Nature* **315,** 474–477 (1985).
10. Kubalek, E. *et al. J. Cell Biol.* **105,** 9–18 (1987).
11. Unwin, P. N. T., Toyoshima, C. & Kubalek, E. *J. Cell Biol.* **107,** 1123–1138 (1988).
12. Sealock, R. *J. Cell Biol.* **92,** 514–522 (1982).
13. Sealock, R., Wray, B. E. & Froehner, S. C. *J. Cell Biol.* **98,** 2239–2244 (1984).
14. Sobel, A. *et al. Proc. natn. Acad. Sci. U.S.A.* **75,** 510–514 (1978).
15. LaRochelle, W. J. & Froehner, S. C. *J. biol. Chem.* **261,** 5271–5274 (1986).
16. Carr, C., McCourt, D. & Cohen, J. B. *Biochemistry* **26,** 7090–7102 (1987).
17. Barrantes, F. J. *J. Cell Biol.* **92,** 60–68 (1982).
18. Neubig, R. R. *et al. Proc. natn. Acad. Sci. U.S.A.* **76,** 690–694 (1979).
19. Toyoshima, C. & Unwin, P. N. T. *Ultramicroscopy* **25,** 279–292 (1988).
20. Caspar, D. L. D. & Kirschner, D. A. *Nature new Biol.* **231,** 46–52 (1971).
21. Lepault, J., Pattus, F. & Martin, N. *Biochim. biophys. Acta* **820,** 315–318 (1985).
22. *International Tables for X-ray Crystallography* Vol. 3 (Reidel, Holland, 1983).
23. Popot, J.-L. *et al. Eur. J. Biochem.* **85,** 27–42 (1978).
24. Bridgman, P. *et al. J. Cell. Biol.* **105,** 1829–1846 (1987).
25. Porter, S. & Froehner, S. C. *J. biol. Chem.* **258,** 10034–10040 (1983).
26. Froehner, S. C. *Trends Neurosci.* **9,** 37–41 (1986).
27. Hille, B. *Ionic Channels of Excitable Membranes* (Sinauer, Sunderland, 1984).
28. Dani, J. A. & Eisenman, G. *J. gen. Physiol.* **89,** 959–983 (1987).
29. DeRosier, D. J. & Moore, P. B. *J. molec. Biol.* **52,** 355–369 (1970).
30. Popot, J.-L. & Changeux, J.-P. *Physiol. Rev.* **64,** 1162–1239 (1984).
31. Bonini, I. C. *et al. Biochem. J.* **245,** 111–118 (1987).